Published in final edited form as:
Cancer Cell. 2007 October ; 12(4): 381–394.

Mutually exclusive inactivation of DMP1 and ARF/p53 in lung cancer

Ali Mallakin[1,2,†], **Takayuki Sugiyama**[1,2], **Pankaj Taneja**[1,2,#], **Lauren A. Matise**[1,2,#], **Donna P. Frazier**[1,2], **Mayur Choudhary**[1,2], **Gregory A. Hawkins**[3], **Ralph B. D'Agostino Jr.**[4], **Mark C. Willingham**[1], and **Kazushi Inoue**[1,2*]

1*The Department of Pathology, Wake Forest University Health Sciences, Medical Center Boulevard, Winston-Salem, NC 27157*

2*The Department of Cancer Biology, Wake Forest University Health Sciences, Medical Center Boulevard, Winston-Salem, NC 27157*

3*Division of Human Genomics, Wake Forest University Health Sciences, Medical Center Boulevard, Winston-Salem, NC 27157*

4*Department of Biostatistical Science, Wake Forest University Health Sciences, Medical Center Boulevard, Winston-Salem, NC 27157*

Summary

Dmp1 (Dmtf1) is activated by oncogenic Ras-Raf-signaling and induces cell cycle arrest in an Arf, p53-dependent fashion. The survival of *K-ras*^{LA} mice was shortened by ~15 weeks in both *Dmp1*$^{+/-}$ and *Dmp1*$^{-/-}$ backgrounds, the lung tumors of which showed significantly decreased frequency of *p53* mutations compared to *Dmp1*$^{+/+}$. Approximately 40 % of *K-ras*^{LA} lung tumors from *Dmp1*$^{+/+}$ mice lost one allele of the *Dmp1* gene, suggesting the primary involvement of *Dmp1* in *K-ras*-induced tumorigenesis. Loss of heterozygosity (LOH) of the h*DMPI* gene was detectable in ~35 % of human lung carcinomas, which was found in mutually exclusive fashion with LOH of *INK4a/ARF* or that of *P53*. Thus, DMP1 is a pivotal tumor suppressor for both human and murine lung cancers.

Keywords

Dmp1; K-ras; p19^{Arf}; p16^{Ink4a}; p53; lung cancer; loss of heterozygosity; deletion; promoter hypermethylation; haploid insufficiency

Significance

Dmp1 (Dmtf1) is activated by oncogenic Ras signaling and shows its tumor suppressor activity through the activation of the Arf-p53 pathway in mice. Here we show that *Dmp1* deletion cooperates with oncogenic *K-ras* to form lung cancers *in vivo* and those tumors from *Dmp1*-knockout mice have significantly less frequent *p53* mutations. Importantly, deletion of one

*Corresponding author, Phone: 336-716-5863; FAX: 336-716-6757; E-mail: kinoue@wfubmc.edu.
†Present address: Department of Dermatology and Skin Science, University of British Columbia, Jack Bell Research Centre, Vancouver, BC Canada V6H 3Z6
#Equal contribution

allele of *Dmp1* was found in 30~40 % of *K-ras*-induced murine lung tumors as well as in human non-small cell lung carcinomas, in which *ARF* and/or *P53* remained intact. The present work provides evidence that *h*DMP1 is a physiological regulator of the ARF-P53 pathway in humans and is primarily involved in pulmonary carcinogenesis.

Introduction

Lung cancer is the leading cause of cancer deaths in the world, and accounts for more solid tumor deaths than any other carcinomas. More than 170,000 new cases are diagnosed each year in the United States alone, of whom ~160,000 will eventually die, representing 30 % of all cancer deaths (Jemal et al., 2006). Lung cancer can be categorized into two major histopathological groups: non-small-cell lung cancer (NSCLC) (Spira and Ettinger, 2004; Moran, 2006) and small-cell lung cancer (SCLC) (Schiller, 2001), the latter of which show neuroendocrine features. Approximately 80 % of lung cancers are NSCLC, and they are subcategorized into adenocarcinomas, squamous cell, adenosquamous, and large-cell carcinomas (Travis, 2002). SCLC and NSCLC show major differences in histopathologic characteristics that can be explained by the distinct patterns of genetic alterations found in both tumor classes (Zochbauer-Muller et al., 2002). For instance, the *K-Ras* gene is mutated in 20~30 % of NSCLC while its mutation is rare in SCLC; *Rb* inactivation is found in ~90 % of SCLC while $p16^{INK4a}$ is inactivated by deletion and/or promoter hypermethylation in ~50 % of NSCLC (for reviews, Fong et al., 2003; Meuwissen and Berns, 2005; Wistuba et al., 2001). Among dozens of the murine models of human lung cancer, the $K\text{-}ras^{LA/+}$ ($K\text{-}ras^{LA1/+}$, $K\text{-}ras^{LA2/+}$) mouse model is one of the most sophisticated ones that mimic human NSCLC (Johnson et al., 2001). In this model, the *K-ras* gene is controlled by its own promoter and is activated only during spontaneous recombination events in the whole animal. Abnormality of the *P53* gene is one of the most common events in human lung cancers (Toyooka et al., 2003), and accordingly, $K\text{-}ras^{LA/+}$ lung carcinogenesis was strikingly accelerated in mice of both $p53^{+/-}$ and $p53^{-/-}$ backgrounds (Johnson et al., 2001).

The activity of p53 is positively regulated by $p19^{Arf}$ ($p14^{ARF}$ in humans) in response to oncogenic stress (Lowe and Sherr, 2003; Sherr 2001, 2006). $p19^{Arf}$ is an alternative reading frame gene product generated from the *Ink4a/Arf* locus which also encodes the cyclin-dependent kinase inhibitor $p16^{Ink4a}$. $p19^{Arf}$ directly binds to Mdm2, thereby stabilizing and activating p53, whereas $p16^{Ink4a}$ binds to cyclin-dependent kinase 4 to inhibit Rb phosphorylation (Kim and Sharpless, 2006; Lowe and Sherr, 2003; Sherr, 2001). Since this single genetic locus encodes two independent tumor suppressor proteins that regulate the p53 and the Rb pathways, it is very frequently disrupted in human cancer (Ruas and Peters, 1998). *Arf* is induced by potentially harmful growth-promoting signals stemming from overexpression of various oncoproteins (Lowe and Sherr, 2003; Sherr, 2001). This Arf induction forces early-stage cancer cells to undergo p53-dependent and p53-independent cell cycle arrest or apoptosis, providing a powerful mode of tumor suppression. The *Arf* promoter monitors latent oncogenic signals *in vivo* (Zindy et al., 2003), and thus *Arf*-null mice are highly prone to spontaneous tumor development (Kamijo et al., 1999). There is a body of evidence showing the p53-independent functions of Arf (reviewed in Sherr, 2006). In human lung cancers, $p14^{ARF}$ is inactivated in 65 % of SCLC, while the gene is deleted in ~20 % of NSCLC. Promoter hypermethylation of *ARF* has been reported in ~10 % of NSCLC, but is less frequent than that of $p16^{INK4a}$ (~40 %) on the same locus (Meuwissen and Berns, 2005). The *Arf* transcription is negatively regulated by overexpression of nuclear proteins such as Bmi1, Twist, Tbx-2/3, and Pokemon, and overexpression of these proteins have been reported in human cancers (Brummelkamp et al., 2001; Maeda et al., 2005; Maestro et al., 1999; Jacobs et al., 1999, 2000; Yang et al., 2004).

Among known *Arf* activators, Dmp1 (cyclin D binding myb-like protein-1; also called Dmtf1: cyclin D binding myb-like transcription factor 1) is a unique tumor suppressor (Hirai and Sherr, 1996; Inoue and Sherr, 1998; for review, Inoue et al., 2007). Dmp1 was originally isolated in a yeast two-hybrid screen of a murine T-lymphocyte library with cyclin D2 as bait (Hirai and Sherr, 1996). Although Dmp1 is structurally related to Myb-family proteins, it binds to nonameric CCCG(G/T)ATG(T/C) DNA consensus sequences, a subset of which is also recognized by proteins of the Ets family. Importantly, Dmp1 directly binds to the *Arf* promoter to activate its expression, thereby inducing p53-dependent cell cycle arrest (Inoue et al., 1999). *Dmp1*-null mice are prone to spontaneous tumor development, which was accelerated when the animals were neonatally treated with ionizing radiation or dimethylbenzanthracene (Inoue et al., 2000, 2001). Lung adenomas/adenocarcinomas were the most common tumors found in *Dmp1*-knockout mice. The retention and expression of the wild-type *Dmp1* allele in tumors arising in heterozygotes indicated that *Dmp1* is haplo-insufficient for tumor suppression (Inoue et al., 2001; for reviews, Quon and Berns, 2001). The low frequency of *Arf* deletion and *p53* mutation in tumors from *Dmp1*-knockout mice suggested that Dmp1 is a physiological regulator of the Arf-p53 pathway *in vivo* (Inoue et al., 2001). Information about the signaling cascades that regulate Dmp1 has been accumulating. The *Dmp1* promoter is activated by the oncogenic Ras-Raf-MEK-ERK-Jun pathway, and the induction of *Arf* by Ras is Dmp1-dependent (Sreeramaneni et al., 2005). On the other hand, the *Dmp1* promoter is repressed by overexpression of E2Fs and also by physiological mitogenic signaling. Thus, Dmp1 is a marker of cells that have exited from the cell cycle (Mallakin et al., 2006). Our recent study shows that the *Dmp1* promoter is repressed by genotoxic stimuli that activate NF-κB (Taneja et al., 2007).

In striking contrast to the accumulating information on murine Dmp1, very little is known about the involvement of *human* DMP1 (*h*DMP1; *h*DMTF1) in cancer. The *h*DMP1 protein has very high structural homology with its murine counterpart (95 % identity with murine Dmp1 at the protein level). One allele of the genes at the h*DMP1* locus was reportedly deleted in all the leukemic cells with chromosome 7q abnormalities regardless of the detailed karyotype at 7q, suggesting that one allelic loss of h*DMP1* could contribute to 7q- malignancies that are refractory to conventional chemotherapy (Bodner et al., 1999). It has been reported that the h*DMP1* locus encodes at least three splicing variants, h*DMP1*α β and γ (Tschan et al., 2003). The full-length h*DMP1*α gene corresponds to the murine *Dmp1* gene that positively regulates the $p19^{Arf}$-p53 pathway (Inoue et al., 1999; Tschan et al., 2003). By contrast, the *h*DMP1β and γ proteins do not bind to DNA and *h*DMP1β has dominant-negative effect on *h*DMP1α when it is overexpressed (Tschan et al., 2003).

Although Dmp1 plays critical roles as a mediator of ras signaling to *Arf* induction in cultured cells, the role of Dmp1 in ras signaling has not been demonstrated *in vivo*. This study was conducted to demonstrate the collaborative effects of *Dmp1* inactivation and *K-ras* activation in pulmonary carcinogenesis. We found that one allele of *Dmp1* was deleted in a significant percentage of lung tumors from $Dmp1^{+/+}$; $K\text{-}ras^{LA}$ mice, showing the primary role of Dmp1 in murine lung cancer. We also analyzed 51 human NSCLC samples for h*DMP1*, *INK4a/ARF*, and *P53* and show that LOH of the h*DMP1* gene is frequently found in NSCLC, especially those which retain an intact *INK4a/ARF* and/or *P53* locus.

Results

$K\text{-}ras^{LA}$ induced tumorigenesis is significantly accelerated in both $Dmp1^{-/-}$ and $Dmp1^{+/-}$ mice

In order to investigate the cooperation of *Dmp1*-inactivation and *K-ras* activation *in vivo*, we backcrossed *Dmp1*-knockout mice for six generations with a C57BL/6 male, and then crossed the $Dmp1^{+/-}$ mice with $K\text{-}ras^{LA2/+}$ or $K\text{-}ras^{LA1/+}$ mice (Johnson et al., 2001). The average

survival of wild-type *K-ras*^{LA} mice was 10–15 weeks longer in our C57BL/6 strain than in the original report due to the difference of the genetic background. *K-ras*$^{LA2/+}$ induced tumorigenesis was greatly accelerated in both *Dmp1*$^{-/-}$ and *Dmp1*$^{+/-}$ mice, with no differences between groups of *Dmp1*$^{-/-}$ and *Dmp1*$^{+/-}$ (Figure 1A; mean survival, 21 weeks in *Dmp1*$^{-/-}$ and *Dmp1*$^{+/-}$ vs. 35 weeks in *Dmp1*$^{+/+}$, $P < 0.005$ in both cases). *K-ras*$^{LA1/+}$ induced tumor formation was also accelerated in both *Dmp1*$^{-/-}$ and *Dmp1*$^{+/-}$ backgrounds (mean survival, 36 weeks in *Dmp1*$^{-/-}$ ($P < 0.001$), 41 weeks in *Dmp1*$^{+/-}$ ($P = 0.001$), and 55 weeks for *Dmp1*$^{+/+}$) (Figure 1B). Although the average survival was slightly shorter in *Dmp1*$^{-/-}$*; K-ras*$^{LA1/+}$ mice than in *Dmp1*$^{+/-}$*; K-ras*$^{LA1/+}$ mice, there was no statistically significant differences between these two cohorts ($P = 0.13$). All of the *K-ras*^{LA} mice generated lung tumors (adenomas and adenocarcinomas) regardless of the *Dmp1* genotype, with minor differences in the incidence of thymic lymphomas (~30 %) and tail papillomas (20~30 %) (Figure S1A). Some of the *Dmp1*$^{+/-}$, *Dmp1*$^{-/-}$*; K-ras*$^{LA/+}$ mice developed other types of tumors than lung carcinomas, thymus lymphomas, or papillomas. They included a case of cholangiocarcinoma, osteosarcoma, neurofibrosarcoma, and ovarian tumor (Figure S1; a picture of cholangiocarcinoma is shown in Figure 2E). Lung tumors from *Dmp1*$^{+/-}$*; K-ras*$^{LA1/+}$ and *Dmp1*$^{+/-}$*; K-ras*$^{LA2/+}$ mice retained the wild-type *Dmp1* allele, when examined by genomic DNA PCR (Figure 1C). The levels of *Dmp1* mRNA expression was 2–5 times higher in 8 of 11 lung tumors from *Dmp1*$^{+/+}$*; K-ras*^{LA} mice than in normal lungs, suggesting the activation of the endogenous *Dmp1* promoter by oncogenic *K-ras* (Figure 1D, middle left panel, gray bars). However, the *Dmp1* mRNA levels were at comparable levels in 3 of 11 *Dmp1*$^{+/+}$*; K-ras*^{LA} lung tumors, suggesting the disruption of the ras-Dmp1 signaling pathway (Figure 1D, middle left panel, white bars). Likewise, the level of *Dmp1* mRNA was 2–4 times higher in 6 of 11 *Dmp1*$^{+/-}$*; K-ras*^{LA} lung tumors than in *Dmp1*$^{+/-}$ lungs while they were at the same or lower levels in 5 of 11 cases (Figure 1D, middle right panel). Nucleotide sequencing of *Dmp1* RT-PCR products from five lung tumors from different mice identified no mutation of *Dmp1* in the DNA-binding domain (data not shown). Immunohistochemical staining of *Dmp1*$^{+/-}$ lung carcinomas with Dmp1-specific antibody (RAX; Mallakin et al., 2006) showed that Dmp1 protein is expressed in lung tumor cells from a *Dmp1*$^{+/-}$*; K-ras*^{LA} mice (Figure 1E, F, and G). These data indicate haploid insufficiency of Dmp1 in suppressing *K-ras*-induced tumor formation.

Biological features of *Dmp1*$^{+/-}$ and *Dmp1*$^{-/-}$ lung tumors

All *K-ras*^{LA} mice developed multi-focal lung tumors when they showed signs of distress and were sacrificed, regardless of the *Dmp1* genotype (Figure 2A–C; Figure S1). Lung carcinomas were found in more than half of *Dmp1*$^{+/-}$ or *Dmp1*$^{-/-}$*; K-ras*^{LA} mice and were significantly larger than those found in *Dmp1*$^{+/+}$ mice of the same age (Figure 2A–C; all the mice were ~40 weeks old). It was common to find nearly entire replacement of the lung by tumors in *Dmp1*$^{+/-}$ or *Dmp1*$^{-/-}$ lung tumors (Figure 2B, C). The number of lung tumor nodules significantly increased in both *Dmp1*$^{+/-}$ and *Dmp1*$^{-/-}$ mice when the mice became sick and sacrificed ($P = 0.008$ and $P = 0.016$, respectively; Figure 2F). Also a trend toward increased nodule size was seen in both *Dmp1*$^{+/-}$ and *Dmp1*$^{-/-}$ mice; however, the difference was not statistically significant due to relatively large variation of tumor size ($P = 0.093$ and $P = 0.077$, respectively). Two of 36 *Dmp1*$^{+/-}$*; K-ras*$^{LA2/+}$ mice and 2 of 38 *Dmp1*$^{+/-}$*; K-ras*$^{LA1/+}$ developed macroscopically recognized distant metastases (three liver/intra-abdominal metastases and one leg metastasis) of their lung tumors (Figure 2D, leg metastasis; Figure 2J, liver metastasis), while none of 50 *Dmp1*$^{+/+}$*; K-ras*$^{LA/+}$ mice showed macroscopic metastatic lesions. The leg or abdominal tumors were negative for markers of carcinoid tumors (chromogranin, synaptophysin), but were positive for a marker for the lung surfactant protein C (Figure S2), indicating that they were metastases of the lung adenocarcinomas. When examined under the light microscope, tumors from *Dmp1*$^{+/+}$*; K-ras*^{LA} mice were adenomas or well-differentiated adenocarcinomas that mimic human papillary adenocarcinomas (~20 %

when the largest lung tumor nodules were studied) (Figure 2G). Approximately 50 % of the largest lung tumors from *Dmp1*$^{+/-}$ or *Dmp1*$^{-/-}$ mice were well, moderately, or poorly differentiated adenocarcinomas, many of which showed signs of intravascular (Figure 2H) or intrabronchial invasion (Figure 2I). There was a trend of increased frequency of intravascular or intrabronchial invasion in *Dmp1*$^{+/-}$ (8/28, 28.6 %) or *Dmp1*$^{-/-}$ (6/16, 37.5 %); *K-ras*^{LA} lung tumors than in *Dmp1*$^{+/+}$*; K-ras*^{LA} lung tumors (4/22, 18.2 %) when they became sick and sacrificed. However, the difference was not statistically different ($P = 0.244$ for *Dmp1*$^{+/-}$ vs. *Dmp1*$^{+/+}$ and $P = 0.102$ for *Dmp1*$^{-/-}$ vs. *Dmp1*$^{+/+}$, respectively) possibly because *Dmp1*$^{+/+}$*; K-ras*^{LA} mice lived 14–19 weeks longer than *Dmp1*$^{+/-}$ or *Dmp1*$^{-/-}$*; K-ras*^{LA} mice (Figure 1A, B), and by that time many of *Dmp1*$^{+/+}$*; K-ras*^{LA} lung tumors have corrupted the Dmp1-p53 pathway (see the following molecular analyses).

p53 mutation is rare in lung tumors from *Dmp1*$^{+/-}$ or *Dmp1*$^{-/-}$*; K-ras*$^{LA/+}$ mice

Previous work had suggested that Dmp1 is a physiological regulator of the Arf-Mdm2-p53 tumor surveillance pathway in Eμ-*Myc* lympholeukemias (Inoue et al., 2001). Thus we studied the frequency of *p53* mutations, Mdm2 overexpression, and *Ink4a/Arf* deletions in *Dmp1* wild-type *K-ras*^{LA} lung carcinomas. p53 was highly (#356, #59, and #844) or moderately (#208) overexpressed in 4 of 11 *Dmp1*$^{+/+}$ lung tumors (36 %) randomly chosen for analysis (Figure 3A). These patterns of p53 protein expression are typical of mutant forms of p53, which neither transcriptionally activate *Mdm2* to trigger p53 destruction (Haupt et al., 1997; Kubbutat et al. 1997) nor repress *Arf* transcription (Stott et al. 1998). Cloning and sequencing of the cDNA for *p53* demonstrated the existence of mutations within the DNA-binding domain in all the four lung cancer samples that overexpressed p53 (data not shown). Three *Dmp1*$^{+/+}$*; K-ras*$^{LA/+}$ lung tumors expressed significant levels of p19^{Arf} (#356, #59, #844), suggesting the disruption of the p53-Arf feedback loop in these tumors. On the other hand, none of the *Dmp1*$^{+/-}$ or *Dmp1*$^{-/-}$*; K-ras*$^{LA/+}$ lung tumors showed high levels of expression of p53, suggesting that the vast majority of the p53 protein expressed in *Dmp1*-knockout tumors was wild-type (Figure 3A, top panels). p19^{Arf} was not upregulated in any of the *Dmp1*$^{+/-}$, *Dmp1*$^{-/-}$*; K-ras*$^{LA/+}$ lung tumors, consistent with the wild-type p53 expression in these tumors (Figure 3A, third panels). Mdm2 was not overexpressed in any of the *K-ras*^{LA} lung tumors compared with the murine cell line that overexpresses Mdm2 (Figure 3A, second panels). None of the *p53, Arf*, or *Ink4a* genes showed biallelic deletion in any of the lung tumors examined, regardless of their *Dmp1* status as studied by semi-quantitative PCR analyses (representative data for *Arf* Exon 1β are shown in Figure 3B; for *p16*^{Ink4a} and *p53*, data not shown). However, *Arf* was hemizygously deleted in ~25 % of *K-ras*^{LA} lung tumors irrespective of the *Dmp1* genotype as studied by real-time PCR (Figure S3A). The *Ink4a/Arf* modulators, Bmi1, Twist, Tbx2/3, and Pokemon have been reported to downregulate p19^{Arf} levels and contribute to tumor formation. However, none of these proteins was overexpressed in *K-ras*^{LA} lung tumors in comparison to 3T3 cells as examined by Western blotting with specific antibodies (Figure S3B).

Since neither homozygous *Arf* deletion nor *Arf* repressor overexpression was found in lung tumors from *Dmp1*$^{+/+}$*; K-ras*$^{LA/+}$ mice, we hypothesized that the *Dmp1* gene might be deleted in some of these lung tumors. Quantitative real-time PCR showed that 5 of 12 lung tumors from *Dmp1* wild-type mice showed single allelic deletion of the *Dmp1* gene (#465, #381, #154, #395, and #205) (Figure 3C, white bars). Interestingly, 5 of 8 (63 %) *p53* wild-type lung tumors showed deletion of the *Dmp1* gene, while none of the *p53*-mutant lung tumors showed hemizygous deletion of *Dmp1* (#356, #59, #208, and #844) (Figure 3C; $P = 0.038$, $\chi^2 = 4.29$). The *Dmp1* locus was selectively deleted in *K-ras*^{LA} lung tumors in most cases since the *gram3* gene located ~430 kb upstream of the *Dmp1* locus was deleted in only one of 12 *K-ras*^{LA} lung tumors and the *abcb1* gene located ~430 kb downstream from the *Dmp1* locus was never deleted in any of the 12 lung tumors (Figure S4). The *Dmp1* gene was not deleted in any

of the lung tumor DNAs isolated from *p53*$^{+/-}$*; K-ras*^{LA} or *p53*$^{-/-}$*; K-ras*^{LA} mice, showing mutually exclusive inactivation of *Dmp1* and *p53* in *K-ras*^{LA} lung tumors (Figure 3D). Collectively, our data indicate that when lung carcinomas arise from wild-type *K-ras*^{LA} mice, the cells undergo either *p53* mutation or *Dmp1* deletion to inactivate the Arf-p53 pathway.

Loss of heterozygosity (LOH) and promoter hypermethylation analyses of h*DMP1* in human non-small cell lung cancer (NSCLC)

The h*DMP1* gene is located on human chromosome 7q21, a region which is often deleted in therapy-induced acute leukemias and myelodysplastic syndromes (Bodner et al., 1999). Whether the human *DMP1* gene (h*DMP1*) is inactivated in human carcinomas has never been investigated. We therefore extracted genomic DNA from 51 non-small cell lung cancer samples (33 adenocarcinomas, 16 squamous cell carcinomas, and 2 adenosquamous carcinomas) and studied LOH for h*DMP1* with two different sets of primers that amplify the dinucleotide repeats located at the 5' (#92465, 34 kb from h*DMP1*) and 3' ends of the h*DMP1* gene (#198004, 28 kb from h*DMP1*; Figure 4A). For *INK4a/ARF* LOH analysis, we designed primers that amplify the repetitive sequences within 500 bps from human *ARF* Exon 1β (#33647) and those that amplify the sequences between Exon 1β and Exonα (#27251;Figure 4B). There are at least 4 high-affinity *h*DMP1 binding sites in this region (Figure 4B, inverted red triangles). For *P53*, two sets of primers were selected that amplify the dinucleotide repeats located 26 kb 5' (#158111) and 11 kb 3' (#89737) of the *P53* gene (Figure 4C). Two major area peaks were quantified from paired samples (normal tissue and lung cancer) and the qLOH values were calculated (see equation described in the Experimental Procedures). When the qLOH values were more than 2.0 or less than 0.5 with either one of the two sets of LOH primers, the tumor sample was found to have LOH for the locus (Figure 4 and Figure 5). Typical cases of LOH positive samples are shown in Figure 4D and E for h*DMP1* (with #92465 and #198004 primer sets), Figure 4F and G for *INK4a/ARF* (with #33647 and #27251), and Figure 4H and I for *P53* (with #158111 and #89737). We also conducted h*DMP1*, *p14*^{ARF}, and *p16*^{INK4a} promoter hypermethylation assays (Figure 5 and Figure S5). The sequences of primers for LOH and promoter hypermethylation assays are shown in Table S1.

With the 5' set of h*DMP1* primers (#92465), 14 of 42 cases (33.3 %) were positive for LOH; with the 3' set of h*DMP1* primers (#198004), 13 of 36 cases were positive (36.1 %). Seven of 29 cases (24.1 %) were positive for LOH with both of these h*DMP1* primer sets (Figure 5). We then conducted detailed mapping of the genomic locus on human chromosome 7q21 deleted in human NSCLC with 5 other sets of LOH primers (Figure 6A). We also conducted quantification of the h*DMP1* genomic DNA at exons 8 and 20 by real-time PCR to supplement the LOH study (Figure 6A, B). Interestingly, the genomic region deleted in NSCLC was confined to the h*DMP1/MGC4175* locus (i.e., from #69164 to #259145) in 15 of 19 h*DMP1* LOH(+) cases (Figure 6B, #2000-3 was not included). Thus, the h*DMP1/MGC4175* locus was specifically targeted in NSCLC samples although there were a small number of cases that showed broader deletion including the h*DMP1/MGC4175* locus.

Next we conducted h*DMP1* promoter methylation assay by using enzymatically methylated human genomic DNA as a positive control. We found only one case of h*DMP1* promoter hypermethylation (#2000-3; Figure 5 and Figure S5). We then isolated RNAs from lung cancer samples from seven different patients in whom duplicate tumor samples were available and conducted sequencing of the h*DMP1* cDNA. All of the seven samples expressed the h*DMP1* mRNA, but none of them, including those which showed LOH for h*DMP1* (#1999-10, #2005-308, and #2005-522), showed mutations for h*DMP1* (data not shown). We then investigated if lung cancer cells had splicing alterations for h*DMP1* by real-time TaqMan PCR in 11 samples that had been randomly chosen. However, we could not detect any lung cancer-specific overexpression of the h*DMP1β* isoform that has dominant-negative effect on

h*DMP1α* (Figure S6; Tschan et al., 2003). Thus, hemizygous gene deletion was considered to be the major mechanism of h*DMP1* inactivation in NSCLC.

Mutually exclusive deletion of h*DMP1* and *INK4a/ARF, P53* in human NSCLC

The 51 pairs of NSCLC samples pairs were also studied for LOH of *INK4a/ARF* and *P53*. With *INK4a/ARF* primers, 12 of 40 cases (30 %) were positive for LOH or showed biallelic deletion with the #33647 primers, and 16 of 45 samples (35.6 %) were positive for LOH or showed biallelic deletion with #27251 primers (Figure 4 and Figure 5). Ten of 35 cases (28.6 %) showed LOH or homozygous deletion with both sets of the *INK4a/ARF* probe. Promoter hypermethylation was found in 3 cases (3/46, 6.5 %) for $p14^{ARF}$ and 25 cases (25/47, 53.2 %) for $p16^{INK4a}$, compatible with previous reports from other groups (Meuwissen and Berns, 2005) (Figure 5 and Figure S5). Ten cases of the $p16^{INK4a}$ promoter hypermethylation were observed simultaneously with LOH of the locus (Figure 5). Three tumor samples showed homozygous deletion of Exon 1β for $p14^{ARF}$ (#2003-86, #2003-442, and #2003-246). Together, the results suggest that these two genes behaved as classical tumor suppressors in the NSCLC samples. Interestingly, 32 out of 34 cases showed mutually exclusive inactivation of the h*DMP1* and the *INK4a/ARF* loci (94.1 %; 95 % confidence interval, 86.2 % to 100 %; $P = 0.0035$, $\chi^2 = 8.52$ based on mutually exclusive hypothesis) compatible with the cluster of *h*DMP1-binding sites throughout the *INK4a/ARF* locus (Figure 4B). LOH of *P53* was found in 30.4 % (14/46) with 5' primers, 46.2 % (18/39) with 3' primers, and 24.3 % (9/37) with both primers. Sequencing analysis of *P53* cDNAs from six lung cancer samples demonstrated the presence of point mutations of *P53* in LOH(+) samples (#2005-308, #2005-391, #1995-95, and #2005-242), but not in LOH(−) samples (#2005-522, #2005-346), indicating that both alleles of *P53* were inactivated in the lung cancer cells that showed LOH for *P53* (data not shown). Again, LOH of h*DMP1* and that of *P53* tend not to overlap each other (Figure 5, 30/35 = 85.7 % exclusive; 95 % confidence interval, 74.1 % to 97.3 %; $P = 0.027$, $\chi^2 = 4.88$ based on mutually exclusive hypothesis). On the other hand, inactivation of the *INK4a/ARF* locus and that of the *P53* locus was found to actually occur more frequently together rather than mutually exclusively (Figure 5; 14/27, 51.9 % exclusive; 95 % confidence interval, 33.0 % to 70.7 %; $P = 0.0045$, $\chi^2 = 8.08$ against mutually exclusive hypothesis). We then genotyped NSCLC samples for *K-Ras* mutation. Point mutations involving codons 12 or 13 of *K-Ras* were found in 7 of 48 samples analyzed (14.6 %), and 3 of the 7 *K-Ras* mutations were found in h*DMP1* LOH(+) samples (#2000-19, #2006-750, and #2005-83; shown in bold ID in Figure 6). Taken together, LOH of the h*DMP1* gene was found in ~35 % of human NSCLC, especially those that retain a wild-type *INK4a/ARF* and/or *P53* locus and ~15 % of h*DMP1* LOH occurred simultaneously with *K-Ras* mutation.

Detection of the *h*DMP1 protein in human lung cancer samples and growth inhibition of lung cancer cell lines by activated Dmp1:ER

To investigate the consequences of hemizygous h*DMP1* deletion in human NSCLC cells, formalin-fixed, paraffin embedded lung cancer sections were stained with Dmp1-specific antibody, RAX (Mallakin *et al.*, 2006; Figure S7). Strong signals were detectable in the nuclei of *P53*-mutant NSCLC cell line H727, which was dramatically downregulated by infecting the cells with h*DMP1*-specific shRNA retroviruses (Figure S7A–C). Then we randomly chose 9 h*DMP1* LOH(+) and 8 h*DMP1* LOH(−) lung cancers and stained them with the antibody to Dmp1. Positive nuclear staining (grade 3++ to 2+) was obtained in 8 of 8 h*DMP1* LOH(−) lung cancer samples while the staining was very weak (grade 1+/−) or negative (grade 0) in 7 of 9 h*DMP1* LOH(+) lung cancers (Figure S7H). In one case (#2006-171) the *h*DMP1 signal was negative, suggesting the complete inactivation of the *h*DMP1 protein in lung cancer cells. Thus, our immunohistochemistry results are quite consistent with those of h*DMP1* LOH analyses ($P < 0.001$).

We then studied if Dmp1 overexpression inhibits the growth of human NSCLC cell lines with different genetic backgrounds of *ARF* and *P53*. In H460 cells with wild-type *ARF* and *P53*, activation of Dmp1:ER with 4-hydroxytamoxifen (4-HT) (Inoue et al., 1999) efficiently inhibited the growth (Figure 7A, pink line). On the other hand, lung cancer cell lines that lack *INK4a/ARF* (A549) or *P53* (H1299, H358) proliferated exponentially even with activation of Dmp1:ER although their growth was slightly slower than control cells (Figure 7B–D; pink lines, Dmp1:ER virus-infected cells with 4-HT; blue lines, mock-infected cells with 4-HT). Western analysis showed accumulation of p14*ARF*, p53, and its target *h*DM2 and $p21^{Cip1}$ in H460 cells where Dmp1:ER was activated with 4-HT (Figure 7E, left panel). In H1299 cells, only $p14^{ARF}$ increased with stimulation of Dmp1:ER (Figure 7E, right panel). Interestingly, real-time PCR analysis showed that the h*DMP1* gene was hemizygously deleted in H460 cells, but not in other cell lines (data not shown). Together, the results indicate that overexpression of activated Dmp1:ER efficiently inhibits the growth of the human lung cancer cell line that has wild-type *ARF* and *P53*.

Discussion

It has now become clear that the DMP1 transcription factor is primarily involved in both human and murine lung cancer. The h*DMP1* gene is located on human chromosome 7q21, a locus often deleted in human malignancies (Bieche et al., 1992; Kerr et al., 1996; Oriola et al., 2001). One previous report showed that the h*DMP1* locus was lost in 9 out of 9 leukemic cells with chromosome 7q abnormalities as studied by FISH, regardless of the detailed karyotype of leukemic cells (Bodner et al., 1999). However, it was difficult to point to the roles of h*DMP1* in human 7q- leukemias since the probe contained sequences of several other genes as well. In this study, we designed unique primers that specifically amplify the repetitive sequences located within 35 kb of the h*DMP1* gene. Thus, the experimental results dependably reflected the events occurring within the locus. With these probes, we could detect the LOH of the h*DMP1* locus in ~35 % of NSCLC samples, the frequency of which was even close to that of the *INK4a/ARF* or *P53* locus of the same samples (30~45 %). Our detailed analysis showed that the deletion of chromosome 7q21 was limited to the h*DMP1/MGC4175* locus in more than 75% of the samples in human NSCLC. Likewise, in *K-ras*^{LA} lung tumors, the deletion was limited to the *Dmp1/MGC4175* locus in more than 90 % of the cases (Figure S4). It was not possible to distinguish the deletion of h*DMP1* and that of *MGC4175* by LOH analyses since these two genes are too closely located. However, it is very unlikely that *MGC4175* deletion contributes to pulmonary carcinogenesis since it encodes a mitochondrial protein that is associated with taxoland doxorubicin-resistant malignant phenotypes in human cancer cell lines (Duan et al., 2004). Most importantly, our current *K-ras*^{LA}*; Dmp1*-knockout mice model clearly points to the role of *Dmp1*-deletion in pulmonary carcinogenesis since *MGC4175* remains intact in the *Dmp1*-targeting vector (Inoue et al., 2000). Thus, we speculate that h*DMP1* is the critical gene for suppression of pulmonary carcinogenesis located on human chromosome 7q21.

Human *DMP1* promoter hypermethylation was found only in one of the 23 lung cancer samples we examined, and none of them showed bi-allelic deletion of the h*DMP1* gene. The second h*DMP1* allele was expressed and not mutated in the tumor cells that showed LOH, although there was one exceptional case where lung tumor cells showed both LOH and promoter methylation for h*DMP1*. Likewise, splicing alterations that result in the overexpression of the dominant-negative h*DMP1*β isoform was not found in the 11 samples we have randomly analyzed (Figure S6). Generally, promoter hypermethylation or point mutation of the second allele is a feature of classical tumor suppressor genes and is very rare in haplo-insufficient tumor suppressors, such as $p27^{Kip1}$ (Chim et al., 2005; Kibel et al., 2001; for review, Herman and Baylin, 2003). Thus, our data are consistent with our hypothesis that h*DMP1* may be haplo-insufficient for tumor suppression in human lung cancer. On the other hand, 3 of 40 NSCLC

cases showed bi-allelic deletion of *ARF* Exon 1β and 10 of 25 cases of $p16^{INK4a}$ promoter methylation occurred simultaneously with LOH of the *INK4a/ARF* locus (Figure 5), compatible with the concept of *INK4a/ARF* being classical tumor suppressors.

Our data indicate that LOH of the h*DMP1* gene and that of the *INK4a/ARF* locus occurred in mutually exclusive fashion in >90 % of the cases ($P< 0.01$), although there were two exceptional cases that showed inactivation of both the h*DMP1* and the *INK4a/ARF* loci. One possible explanation is that the deletion or methylation of the *INK4a/ARF* locus will result in the absence or modification of the *h*DMP1-binding sites: thus, tumors that have inactivated *INK4a/ARF* do not have to delete the h*DMP1* gene at the same time. Likewise, LOH of h*DMP1* also occurred significantly less frequently in lung tumors that showed LOH for *P53* ($P< 0.05$). Interestingly, one of the four human non-small cell lung cancer cell lines (H460) showed hemizygous deletion of h*DMP1*, where both *ARF* and *P53* are wild-type (Somasundaram et al., 1999) and *K-Ras* is mutant. Activated Dmp1:ER efficiently induced $p14^{ARF}$ and inhibited the growth of H460 cells while other lung cancer cell lines with deletion of *ARF* (A549) or *P53* (H1299, H358) were resistant to Dmp1 overexpression. Consistent with the human data, the *Dmp1* gene was deleted only in $K\text{-}ras^{LA}$ lung tumors with wild-type *p53*, and but not in any of the lung tumors from $p53^{+/-}$ or $p53^{-/-}$; $K\text{-}ras^{LA}$ mice, suggesting the mutually exclusive inactivation of *Dmp1* and *p53* in $K\text{-}ras^{LA}$ lung tumors. Collectively, the *DMP1* gene is frequently deleted in lung tumors where the *INK4a/ARF* locus and/or the *P53* locus remains wild-type since *h*DMP1, ARF, and P53 are in the same signaling pathway.

Although homozygous deletion of *Arf* was not observed in any $K\text{-}ras^{LA}$ lung tumors, hemizygous deletion of *Arf* was found in ~25 % of lung tumors regardless of the genotype of *Dmp1*. Haploid insufficiency of $p19^{Arf}$ has been reported in murine solid tumors only when $p16^{Ink4a}$ was homozygously inactivated (Krimpenfort et al., 2001). However, inactivation of $p16^{Ink4a}$ by gene deletion or promoter hypermethylation is rare in $K\text{-}ras^{LA}$ lung tumors (Johnson et al., 2001; J. Sage, personal communication). Therefore, it is unlikely that the hemizygous *Arf* deletion contributed to lung tumorigenesis. If *Arf* does not contribute to $K\text{-}ras^{LA}$ lung tumors, Dmp1 should be regulating the p53 activity by a yet unknown mechanism. On the other hand, $p14^{ARF}$ is apparently involved in human NSCLC either by 1) biallelic deletion (#2003-86, #2003-442, and #2003-246)(Figure 5) or by 2) hemizygous deletion with simultaneous biallelic inactivation of the $p16^{INK4a}$ locus (#2000-96, #2003-422, #2004-719, #2004-983, #1999-95, and #2006-172).

$K\text{-}ras^{LA}$ lung tumors are different from Eμ-*Myc* lymphomas in that bi-allelic *Arf* deletion or Mdm2 overexpression was not found in any tumors regardless of the genotype of *Dmp1* (Inoue et al., 2001). None of the *Ink4a/Arf* modulators, such as Bmi1, Twist, Tbx2/3, and Pokemon were overexpressed in $K\text{-}ras^{LA}$ lung tumors, ruling out the possibility of the involvement of these *Ink4a/Arf* modulators for *K-ras*-induced tumor formation. *p53* mutation was less frequent in lung tumors from $Dmpl^{+/-}$, $Dmp1^{-/-}$; $K\text{-}ras^{LA}$ mice, thus *Dmp1* deletions and *p53* mutations might have similar effects. In fact, we have found that tumors that showed deletion of *Dmp1* tend to show the phenotype of adenocarcinomas (5/7, 71 %; the number includes two other cases of *Dmp1* deletion that were not shown in Figure 3). All the lung tumors that showed mutation of *p53* were adenocarcinomas (4/4, 100 %). On the other hand, lung tumors that did not show *Dmp1* or *p53* alterations were mostly adenomas, and there was only one case of adenocarcinoma in this group (1/5, 20 %). This phenotypic difference was statistically significant ($P = 0.036$ for *Dmp1* deletion, $P = 0.016$ for *p53* mutation). Thus, deletions of *Dmp1* or mutations of *p53* are frequently associated with malignant phenotypes of $K\text{-}ras^{LA}$ lung tumors.

Dmp1 showed typical haploid insufficiency in suppression of $K\text{-}ras^{LA}$ lung cancers, especially in $K\text{-}ras^{LA2/+}$ tumors. Although many other tumor suppressor genes have now been reported

to show haploid-insufficiency to some extent, this level of strong haploid insufficiency was observed only in *p27*^{Kip1} and *Dmp1* (reviewed in Payne and Kemp, 2006; Quon and Berns, 2001). In the case of p27^{Kip1}, it was explained that complete loss of *p27*^{Kip1} results in decreased assembly of cyclin D1 and Cdk4 especially in mammary epithelial cells, thus MMTV-*neu*-induced breast cancer was not accelerated in a *p27*$^{Kip1-/-}$ background (Muraoka et al., 2002). Although the exact molecular mechanisms of haploid insufficiency of *Dmp1* remain to be determined, apparently one copy loss of *Dmp1* is enough to inactivate the p53 pathway in *K-ras* as well as in Eμ-*Myc*-induced tumor formation (Figure 3A in this study; Inoue et al., 2001).

In conclusion, we have demonstrated that the *Dmp1* (h*DMP1*) gene is hemizygously deleted in a significant percentage of murine and human non-small cell lung carcinomas, especially those which retained the intact Arf-p53 pathway. Thus, DMP1 is principally involved in pulmonary carcinogenesis. Dmp1 showed haploid insufficiency in *K-ras*^{LA} murine lung tumors, and our data with lung cancer patients' samples are compatible with haploid insufficiency of h*DMP1* in NSCLC. Since h*DMP1* LOH (+) lung cancer cells retain one allele of the h*DMP1* locus, this gene might be a promising target for future drug development.

Experimental Procedures

Creation of *Dmp1*$^{+/-}$, *Dmp1*$^{-/-}$; *K-ras*$^{LA/+}$ mice

Dmp1-heterozygous females were backcrossed to the same C57BL/6 male for more than six generations to obtain *Dmp1*$^{+/-}$ mice that were >98 % C57BL/6 background overall. The mouse *Dmp1* gene is localized on chromosome 5. All the seven markers on mouse chromosome 5 had been replaced with the C57BL/6 markers at G6. One male *K-ras*$^{LA1/+}$ or *K-ras*$^{LA2/+}$ mouse was crossed with two *Dmp1*$^{+/-}$ females to obtain *Dmp1*$^{+/-}$; *K-ras*$^{LA1/+}$ or *K-ras*$^{LA2/+}$ mice. Then these *Dmp1*$^{+/-}$; *K-ras*$^{LA/+}$ transgenic mice were further crossed with *Dmp1*$^{+/-}$ mice to obtain more than 25 mice with each genetic background. Mice were observed daily, and were euthanized when they showed any signs of tumor formation. Mice were maintained in accordance with the Guide for the Care and Use of Laboratory Animals.

Statistical analyses

Statistical differences of survival in *Dmp1*$^{+/+}$, *Dmp1*$^{+/-}$, and *Dmp1*$^{-/-}$; *K-ras*$^{LA1/+}$ or *K-ras*$^{LA2/+}$ mice were analyzed by XLSTAT-Life software (Addinsoft, New York, NY). Mann-Whitney test (two-sided) were used to generate the *P values* (significance level, $\alpha = 0.05$). For each comparison of LOH, we performed a 1 degree of freedom test to determine whether the LOH of h*DMP1, INK4a/ARF*, and *P53* in NSCLC samples were more likely to occur mutually exclusively or together. To do this, three separate chi-square tests were performed - one for each pair of data (i.e., h*DMP1* and *INK4a/ARF*, h*DMP1* and *P53*, and *INK4a/ARF* and *P53*). In these analyses, we examined the expected cell count versus the observed cell count in order to determine whether there was evidence of mutual exclusivity or not (evidence of mutual exclusivity is supported when the off-diagonal elements of the 2×2 table have higher observed counts than expected, whereas mutual exclusivity is not supported if the main diagonal cells of the 2×2 table have higher observed counts than expected). In addition to performing chi-square tests, we estimate 95 % confidence intervals for binomial proportions (using a normal approximation). These intervals were calculated using data where at least one of the two markers showed LOH (shown in bold red in Figure 5) and we estimated the probability that co-occurrence does not happen given that at least one marker has occurred. Unpaired Student's *t*-tests were conducted for the analyses of number and size of *K-ras*^{LA} lung tumors as well as to demonstrate the difference of intensity of *h*DMP1 signals in immunohistochemistry.

Human lung cancer samples

Fifty-one pairs of frozen human lung cancer tissues (33 cases of adenocarcinoma, 16 cases of squamous cell carcinoma, and 2 cases of adenosquamous carcinoma) and their normal counterparts were obtained from the Tissue Procurement Core Facility at the Wake Forest University Comprehensive Cancer Center. The samples had already been resected from patients with informed consent and had been stored in liquid nitrogen. The samples do not contain any subject identifiers. The human protocol had been approved by the Institutional Review Board.

Loss of heterozygosity (LOH) and sequencing analyses of human lung cancer specimen

Two sets of markers for microsatellite analysis of h*DMP1* (#92465, #198004), two sets of markers for *INK4a/ARF* (#33647, #27251), and two sets of markers for *P53* (#158111, #89737) were selected by using the software at http://www.gramene.org (Ware et al., 2002) (Figure 4A–C). These markers were chosen because they are polymorphic between individuals in more than 60 % of the cases. For detailed mapping of the region deleted in human NSCLC, 4 other sets of primers were designed by our selves (B-Actin, #69164, #251945, and ABCB1) (Figure 6A, Table S1). D7S644 sequences were obtained from the NCBI. The forward primer of each pair was labeled on the 5' end with the fluorescent dye FAM (Operon Technologies, Huntsville, AL) and PCR amplification was performed with DNA isolated from the tumor and normal tissues. PCR products were visualized on a 1.2 % agarose gel. Genotypes were identified by peak analysis of the fluorescent signal detected on an ABI 3700 DNA analyzer (Applied Biosystems). The qLOH values were determined through the following equation. qLOH = Area Peak 1/Area Peak 2 (normal tissue) divided by Area Peak 1'/Area Peak 2' (tumor tissue). LOH was assessed if the qLOH value was found to be >2.0 or <0.5 (So et al., 2004). Each sample was found to be positive for LOH of the locus when the qLOH values were >2.0 or <0.5 in one of the two sets of primers. When one of the two sets of LOH primers showed a single peak, LOH was determined by the other set. Whenever duplicate samples were available, total RNA was extracted from lung cancer tissues by using RNA*later*®-ICE (Ambion, Applied Biosystems) and TRIzol® (Invitrogen, Carlsbad, CA), and RT-PCR was conducted with *PfuUltra*™ Hotstart DNA polymerase (Stratagene, La Jolla, CA).

Other experimental procedures are described in Supplemental Data.

Supplementary Material

Refer to Web version on PubMed Central for supplementary material.

Acknowledgements

We are very grateful to T. Jacks, D. Tuveson, N. Young, K. Mercer, and A. Deconinck for *K-ras*^{LA} mice and paraffin blocks for *p53*$^{+/-}$, *p53*$^{-/-}$; *K-ras*^{LA} mice; J. Sage for unpublished data; G. Sui and K. Klein and for critical reading of the manuscript. We thank C. Sherr and M. Roussel for *Dmp1*-knockout mice and plasmids. We also thank J. Garvin for murine pathology and J. Clark, S. Lagedrost, and S. Barton for technical assistance. This work was supported by NIH/NCI 5R01CA106314 (K. Inoue). D. Frazier is supported by NIH Institutional Research Training Grant 5T32CA079448 (F. Torti).

References

Bieche I, Champeme MH, Matifas F, Hacene K, Callahan R, Lidereau R. Loss of heterozygosity on chromosome 7q and aggressive primary breast cancer. Lancet 1992;339:139–143. [PubMed: 1346009]

Bodner SM, Naeve CW, Rakestraw KM, Jones BG, Valentine VA, Valentine MB, Luthardt FW, Willman CL, Raimondi SC, Downing JR, et al. Cloning and chromosomal localization of the gene encoding human cyclin D-binding Myb-like protein (*h*DMP1). Gene 1999;229:223–228. [PubMed: 10095122]

Chim CS, Wong AS, Kwong YL. Epigenetic inactivation of the CIP/KIP cell-cycle control pathway in acute leukemias. Am. J. Hematol 2005;80:282–287. [PubMed: 16315255]

Duan Z, Brakora KA, Seiden MV. MM-TRAG (MGC4175), a novel intracellular mitochondrial protein, is associated with the taxol- and doxorubicin-resistant phenotype in human cancer cell lines. Gene 2004;340:53–59. [PubMed: 15556294]

Fong KM, Sekido Y, Gazdar AF, Minna JD. Lung cancer. 9: Molecular biology of lung cancer: Clinical implications. Thorax 2003;58:892–900. [PubMed: 14514947]

Haupt Y, Maya R, Kazaz A, Oren M. Mdm2 promotes the rapid degradation of p53. Nature 1997;387:296–299. [PubMed: 9153395]

Herman JG, Baylin SB. Gene silencing in cancer in association with promoter hypermethylation. New Engl. J. Med 2003;349:2042–2054. [PubMed: 14627790]

Hirai H, Sherr CJ. Interaction of D-type cyclins with a novel myb-like transcription factor. DMP1. Mol. Cell. Biol 1996;16:6457–6467.

Inoue K, Sherr CJ. Gene expression and cell cycle arrest mediated by transcription factor DMP1 is antagonized by D-type cyclins through a cyclin-dependent-kinase-independent mechanism. Mol. Cell. Biol 1998;18:1590–1600. [PubMed: 9488476]

Inoue K, Sherr CJ, Shapiro LH. Regulation of the CD13/aminopeptidase N gene by DMP1, a transcription factor antagonized by D-type cyclins. J. Biol. Chem 1998;273:29188–29194. [PubMed: 9786929]

Inoue K, Roussel MF, Sherr CJ. Induction of *ARF* tumor suppressor gene expression and cell cycle arrest by transcription factor DMP1. Proc. Natl. Acad. Sci. USA 1999;96:3993–3998. [PubMed: 10097151]

Inoue K, Wen R, Rehg JE, Adachi M, Cleveland JL, Roussel MF, Sherr CJ. Disruption of the *ARF* transcriptional activator *DMP1* facilitates cell immortalization, Ras transformation, and tumorigenesis. Genes Dev 2000;14:1797–1809. [PubMed: 10898794]

Inoue K, Zindy F, Randle DH, Rehg JE, Sherr CJ. *Dmp1* is haplo-insufficient for tumor suppression and modifies the frequencies of Arf and p53 mutations in Myc-induced lymphomas. Genes Dev 2001;15:2934–2939. [PubMed: 11711428]

Inoue K, Mallakin A, Frazier DP. Dmp1 and tumor suppression. Oncogene 2007;26:4329–4335. [PubMed: 17237816]

Jacobs JJ, Kieboom K, Marino S, DePinho RA, van Lohuizen M. The oncogene and polycomb-group gene bmi-1 regulates cell proliferation and senescence through the ink4a locus. Nature 1999;397:164–168. [PubMed: 9923679]

Jacobs JJ, Keblusek P, Robanus-Maandag E, Kristel P, Lingbeek M, Nederlof PM, van Welsem T, van de Vijver MJ, Koh EY, Daley GQ, et al. Senescence bypass screen identifies TBX2, which represses Cdkn2a (p19(ARF)) and is amplified in a subset of human breast cancers. Nat Genet 2000;26:291–299. [PubMed: 11062467]

Jemal A, Siegel R, Ward E, Murray T, Xu J, Smigal C, Thun MJ. Cancer statistics, 2006. CA Cancer J. Clin 2006;56:106–130. [PubMed: 16514137]

Johnson L, Mercer K, Greenbaum D, Bronson RT, Crowley D, Tuveson DA, Jacks T. Somatic activation of the *K-ras* oncogene causes early onset lung cancer in mice. Nature 2001;410:1111–1116. [PubMed: 11323676]

Kamijo T, Bodner S, van de Kamp E, Randle DH, Sherr CJ. Tumor spectrum in ARF-deficient mice. Cancer Res 1999;59:2217–2222. [PubMed: 10232611]

Kerr J, Leary JA, Hurst T, Shih YC, Antalis TM, Friedlander M, Crawford E, Khoo SK, Ward B, Chenevix-Trench G. Allelic loss on chromosome 7q in ovarian adenocarcinomas: two critical regions and a rearrangement of the PLANH1 locus. Oncogene 1996;13:1815–1818. [PubMed: 8895529]

Kibel AS, Christopher M, Faith DA, Bova GS, Goodfellow PJ, Isaacs WB. Methylation and mutational analysis of p27(kip1) in prostate carcinoma. Prostate 2001;48:248–253. [PubMed: 11536304]

Kim WY, Sharpless NE. The regulation of *INK4/ARF* in cancer and aging. Cell 2006;127:265–275. [PubMed: 17055429]

Krimpenfort P, Quon KC, Mooi WJ, Loonstra A, Berns A. Loss of p16Ink4a confers susceptibility to metastatic melanoma in mice. Nature 2001;413:83–86. [PubMed: 11544530]

Kubbutat MH, Jones SN, Vousden KH. Regulation of p53 stability by Mdm2. Nature 1997;387:299–303. [PubMed: 9153396]

Lowe S, Sherr CJ. Tumor suppression by *Ink4a-Arf*: Progress and puzzles. Curr. Opin. Genet. Dev 2003;13:77–83. [PubMed: 12573439]

Maeda T, Hobbs RM, Merghoub T, Guernah I, Zelent A, Cordon-Cardo C, Teruya-Feldstein J, Pandolfi PP. Role of the proto-oncogene Pokemon in cellular transformation and ARF repression. Nature 2005;433:278–285. [PubMed: 15662416]

Maestro R, DeiTos AP, Hamamori Y, Krasnokutsky S, Sartorelli V, Kedes L, Doglioni C, Beach DH, Hannon GJ. Twist is a potential oncogene that inhibits apoptosis. Genes Dev 1999;13:2207–2217. [PubMed: 10485844]

Mallakin A, Taneja P, Matise LA, Willingham MC, Inoue K. Expression of Dmp1 in specific differentiated, nonproliferating cells and its repression by E2Fs. Oncogene 2006;25:7703–7713. [PubMed: 16878159]

Meuwissen R, Berns A. Mouse models for human lung cancer. Genes Dev 2005;19:643–664. [PubMed: 15769940]

Moran CA. Pulmonary adenocarcinoma: The expanding spectrum of histologic variants. Arch. Pathol. Lab. Med 2006;130:958–962. [PubMed: 16831050]

Muraoka RS, Lenferink AE, Law B, Hamilton E, Brantley DM, Roebuck LR, Arteaga CL. ErbB2/Neu-induced, cyclin D1-dependent transformation is accelerated in p27-haploinsufficient mammary epithelial cells but impaired in *p27*-null cells. Mol. Cell. Biol 2002;22:2204–2219. [PubMed: 11884607]

Oriola J, Halperin I, Mallofre C, Muntane J, Angel M, Rivera-Fillat F. Screening of selected genomic areas potentially involved in thyroid neoplasms. Eur. J. Cancer 2001;37:2470–2474. [PubMed: 11720845]

Payne SR, Kemp CJ. Tumor suppressor genetics. Carcinogenesis 2006;26:2031–2045. [PubMed: 16150895]

Quon KC, Berns A. Haplo-insufficiency? Let me count the ways. Genes Dev 2001;15:2917–2921. [PubMed: 11711426]

Ruas M, Peters G. The $p16^{INK4a}$/CDKN2A tumor suppressor and its relatives. Biochim. Biophys. Acta Rev. Cancer 1998;1378:F115–F177.

Schiller JH. Current standards of care in small-cell and non-small-cell lung cancer. Oncology 2001;61:3–13. [PubMed: 11598409]

Sherr CJ. The INK4a/ARF network in tumor suppression. Nat. Rev. Mol. Cell. Biol 2001;2:731–737. [PubMed: 11584300]

Sherr CJ. Divorcing ARF and p53: an unsettled case. Nat. Rev. Cancer 2006;6:663–673. [PubMed: 16915296]

So CK, Nie Y, Song Y, Yang GY, Chen S, Wei C, Wang LD, Doggett NA, Yang CS. Loss of heterozygosity and internal tandem duplication mutations of the CBP gene are frequent events in human esophageal squamous cell carcinoma. Clin. Cancer Res 2004;10:19–27. [PubMed: 14734447]

Somasundaram K, MacLachlan TK, Burns TF, Sgagias M, Cowan KH, Weber BL, el-Deiry WS. BRCA1 signals ARF-dependent stabilization and coactivation of p53. Oncogene 1999;18:6605–6614. [PubMed: 10597265]

Spira A, Ettinger DS. Multidisciplinary management of lung cancer. N. Engl. J. Med 2004;350:379–392. [PubMed: 14736930]

Sreeramaneni R, Chaudhry A, McMahon M, Sherr CJ, Inoue K. Ras-Raf-Arf signaling critically depends on Dmp1 transcription factor. Mol. Cell. Biol 2005;25:220–232. [PubMed: 15601844]

Stott FJ, Bates S, James MC, McConnell BB, Starborg M, Brookes S, Palmero I, Ryan K, Hara E, Vousden KH, et al. The alternative product from the human *CDKN2A* locus, $p14^{ARF}$, participates in a regulatory feedback loop with p53 and MDM2. EMBO J 1998;17:5001–5014. [PubMed: 9724636]

Taneja P, Mallakin A, Matise LA, Frazier DP, Choudhary M, Inoue K. Repression of Dmp1 and Arf transcription by anthracyclins: critical roles of the NF-kappaB subunit p65. Oncogene. 2007 Jun 4; [Epub ahead of print]

Toyooka S, Tsuda T, Gazdar AF. The *TP53* gene, tobacco exposure, and lung cancer. Hum. Mutat 2003;21:229–239. [PubMed: 12619108]

Travis WD. Pathology of lung cancer. Clin. Chest Med 2002;23:65–81. [PubMed: 11901921]

Tschan MP, Fischer KM, Fung VS, Pirnia F, Borner MM, Fey MF, Tobler A, Torbett BE. Alternative splicing of the human cyclin D-binding Myb-like protein (hDMP1) yields a truncated protein isoform that alters macrophage differentiation patterns. J. Biol. Chem 2003;278:42750–42760. [PubMed: 12917399]

Yang J, Mani SA, Donaher JL, Ramaswamy S, Itzykson RA, Come C, Savagner P, Gitelman I, Richardson A, Weinberg RA. Twist, a master regulator of morphogenesis, plays an essential role in tumor metastasis. Cell 2004;117:927–939. [PubMed: 15210113]

Wistuba I, Gazdar AF, Minna JD. Molecular genetics of small cell lung carcinoma. Semin. Oncol 2001;28:3–13. [PubMed: 11479891]

Zindy F, Williams RT, Baudino TA, Rehg JE, Skapek SX, Cleveland JL, Roussel MF, Sherr CJ. Arf tumor suppressor promoter monitors latent oncogenic signals in vivo. Proc. Natl. Acad. Sci. USA 2003;100:15930–15935. [PubMed: 14665695]

Zochbauer-Muller S, Gazdar AF, Minna JD. Molecular pathogenesis of lung cancer. Annu. Rev. Physiol 2002;64:681–708. [PubMed: 11826285]

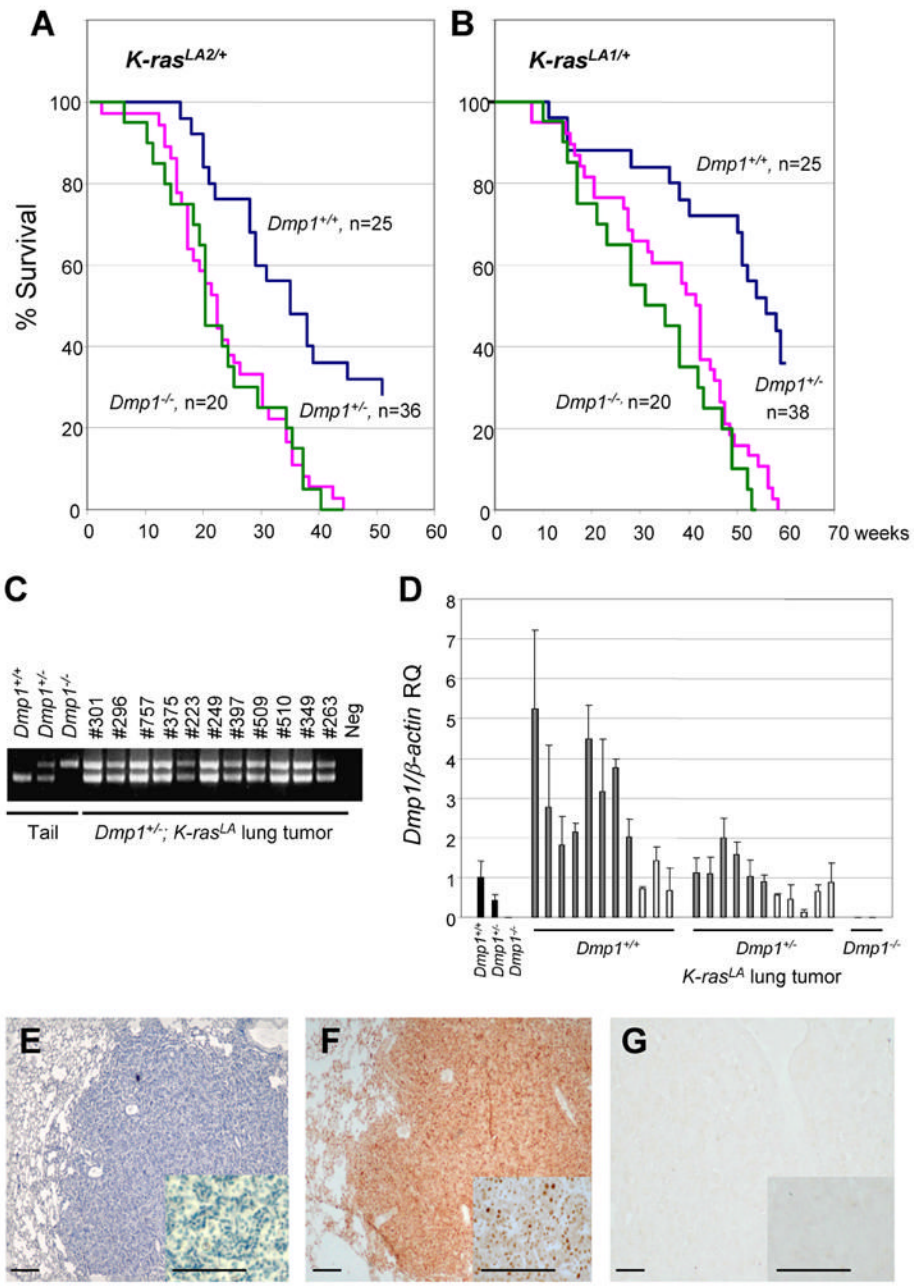

Figure 1. Tumor-free survival in cohorts of (A) *Dmp1*$^{+/+}$, *Dmpl*$^{+/-}$, and *Dmp1*$^{-/-}$; *K-ras*$^{LA2/+}$ mice and (B) *Dmp1*$^{+/+}$, *Dmp1*$^{+/-}$, and *Dmp1*$^{-/-}$; *K-ras*$^{LA1/+}$ mice

A: Statistically significant difference in survival was found between *Dmp1*$^{+/+}$ vs. *Dmp1*$^{+/-}$; *K-ras*$^{LA2/+}$ ($P< 0.005$) and *Dmp1*$^{+/+}$ vs. *Dmp1*$^{-/-}$; *K-ras*$^{LA2/+}$ mice ($P< 0.005$). There were no significant differences in survival between *Dmp1*$^{+/-}$ vs. *Dmp1*$^{-/-}$; *K-ras*$^{LA2/+}$ ($P= 0.38$).
B: Significant difference of survival was found between *Dmp1*$^{+/+}$ vs. *Dmp1*$^{-/-}$; *K-ras*$^{LA1/+}$ ($P< 0.001$) and *Dmp1*$^{+/+}$ vs. *Dmp1*$^{+/-}$; *K-ras*$^{LA1/+}$ mice ($P= 0.001$), but not between *Dmp1*$^{+/-}$ vs. *Dmp1*$^{-/-}$; *K-ras*$^{LA1/+}$ ($P= 0.13$).
C: Retention of the *Dmp1* wild-type allele in lung tumors from *Dmp1*$^{+/-}$; *K-ras*$^{LA/+}$ mice as examined by genomic DNA PCR.

D: Expression of the *Dmp1* mRNA in lung tumors from $Dmp1^{+/+}$, $Dmp1^{+/-}$, and $Dmp1^{-/-}$; $K\text{-}ras^{LA/+}$ mice. Real-time PCR was conducted to quantitate the *Dmp1* mRNA expression in $K\text{-}ras^{LA/+}$ lung tumors. Black bars show the average level of *Dmp1* expression in the lung of each genotype. Gray bars are the samples that showed higher level of *Dmp1* expression in $K\text{-}ras^{LA}$ lung tumors than in their normal lung controls. The means $Dmp1^{+/-}$ SD for three experiments are shown.

E: Well-differentiated lung adenocarcinoma found in a $Dmp1^{+/-}$; $K\text{-}ras^{LA1/+}$ mouse. H&E stain.

F: Detection of the Dmp1 protein in the nuclei of $Dmp1^{+/-}$; $K\text{-}ras^{LA1/+}$ mouse tumor cells with the Dmp1-specific antibody, RAX.

G: Negative staining of the lung tumor section of $Dmp1^{-/-}$; $K\text{-}ras^{LA1/+}$ mouse with RAX antibody. Scale bar in E, F, and G is 100 μm.

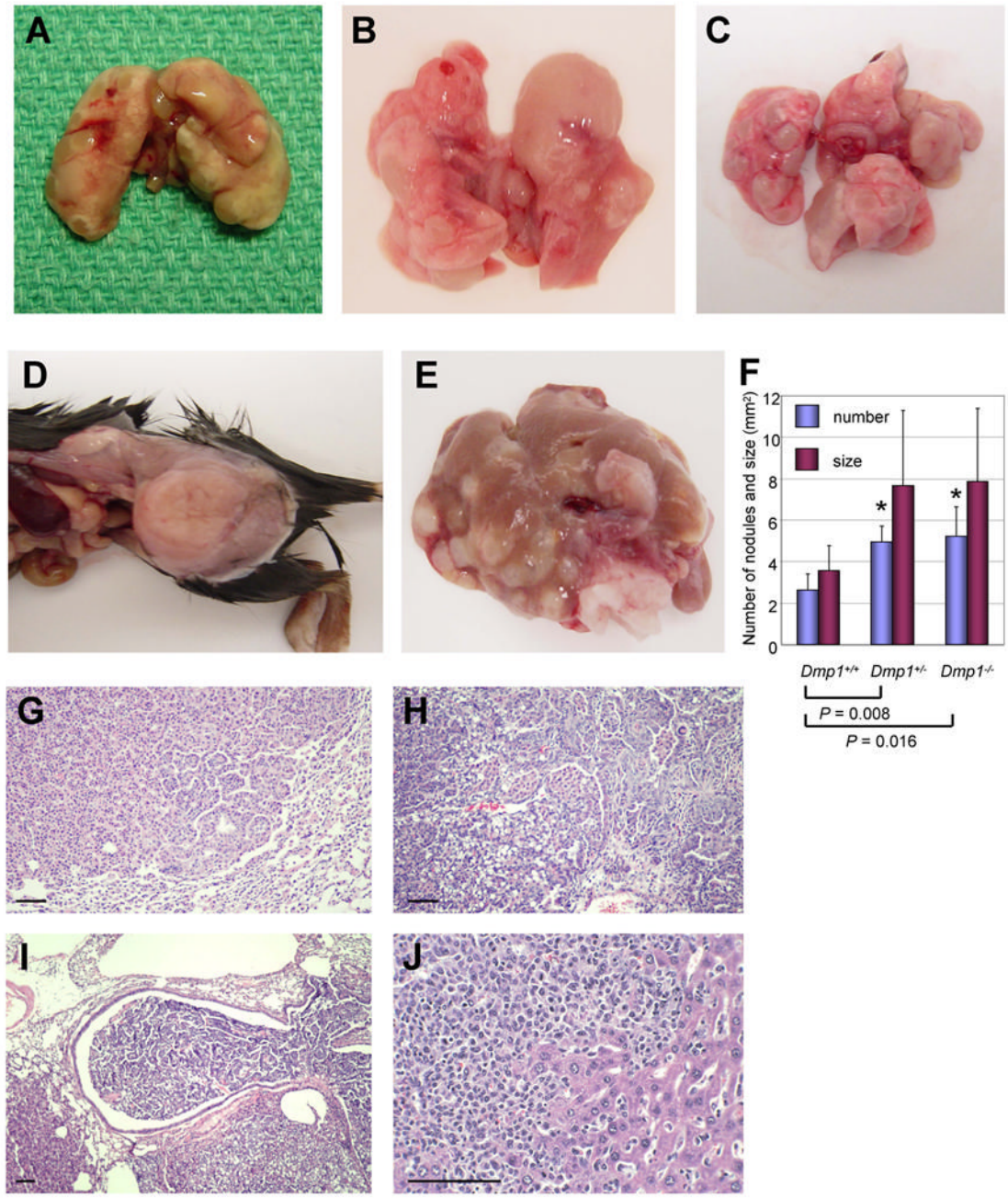

Figure 2. Pathological examination of tumors found in *K-ras*$^{LA/+}$ mice

A: Multiple lung adenomas and adenocarcinomas in a *Dmp1*$^{+/+}$*; K-ras*$^{LA1/+}$ mouse (42-week-old).

B: Advanced lung adenocarcinoma in a *Dmp1*$^{+/-}$*; K-ras*$^{LA1/+}$ mouse (39-week-old).

C: Disseminated lung adenocarcinoma in a *Dmp1*$^{-/-}$*; K-ras*$^{LA1/+}$ mouse (38-week-old).

D: Leg metastasis of lung adenocarcinoma in a *Dmp1*$^{+/-}$*; K-ras*$^{LA1/+}$ mouse (40-week-old).

E: Cholangiocarcinoma of the liver in a *Dmp1*$^{+/-}$*; K-ras*$^{LA1/+}$ mouse (40-week-old).

F: Lung nodule number and size (mean +/− SEM) in *K-ras*^{LA} mice. Ranges were compared with unpaired Student's t-tests.

G: Well-differentiated adenocarcinoma found in a *Dmp1*$^{+/+}$*; K-ras*$^{LA2/+}$ mouse.

H: Poorly differentiated adenocarcinoma in a *Dmp1*$^{+/-}$*; K-ras*$^{LA2/+}$ mouse. The tumor cells are very pleomorphic and are invading into blood vessels.
I: Intrabronchial invasion of a *Dmp1*$^{-/-}$*; K-ras*$^{LA2/+}$ lung carcinoma.
J: Liver metastasis of lung adenocarcinoma in a *Dmp1*$^{+/-}$*; K-ras*$^{LA2/+}$ mouse. Scale bar in G, H, I, and J is 100 μm.

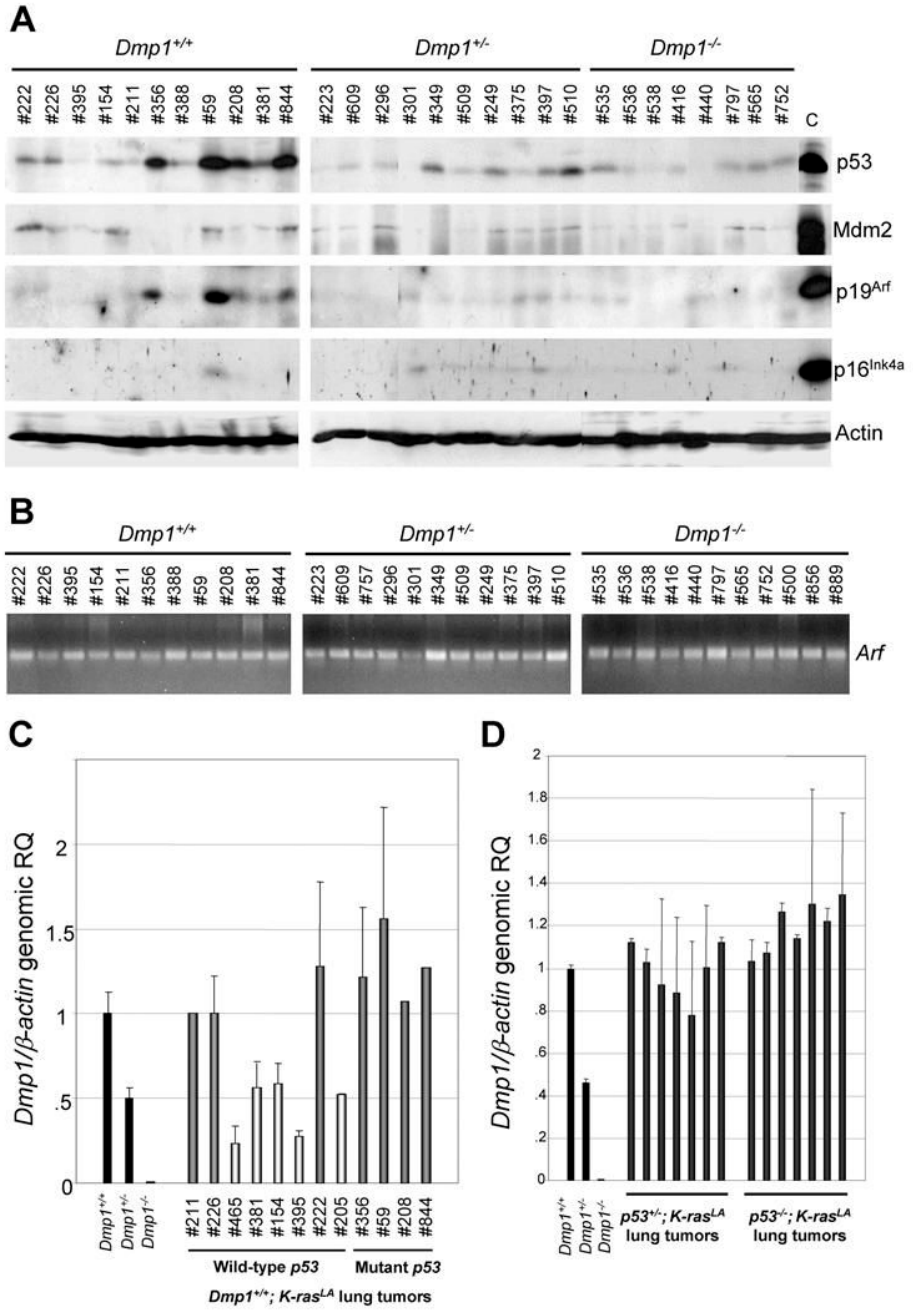

Figure 3.

Analysis of the Arf-Mdm2-p53 pathway in *K-ras*$^{LA/+}$ lung tumors.

A: Western blotting of lung tumors for p53, Mdm2, p19^{Arf}, and p16^{Ink4a}. Tumor cells were resected from the center of well-circumscribed lung carcinomas under the light microscope and proteins were extracted. The control cell lysates were obtained from spontaneously immortalized *p53*-mutant MEFs for p53, p19^{Arf}, p16^{Ink4a}, and Actin; dm3T3 cells for Mdm2. The *p53* mutations were detected in 4 of 11 *Dmp1*$^{+/+}$*; K-ras*$^{LA/+}$ mice (36 %) while they were not found in the *Dmp1*$^{+/-}$ and *Dmp1*$^{-/-}$*; K-ras*$^{LA/+}$ lung tumors.

B: Detection of the p19^{Arf} Exon1β genomic DNA by semi-quantitative-PCR. The *Arf* gene was not homozygously deleted in *K-ras*^{LA} lung tumors regardless of the *Dmp1* genotype.

C: Quantification of the *Dmp1* genomic DNA by real-time PCR. The black bars show the relative copy number of the *Dmp1* genomic DNA in $Dmp1^{+/+}$, $Dmp1^{+/-}$, and $Dmp1^{-/-}$ mice tails, with *β-actin* as an internal control (mean +/− SEM). The *Dmp1* locus is deleted in 5 of 12 randomly chosen lung tumors from $Dmp1^{+/+}$; $K\text{-}ras^{LA/+}$ mice. The *Dmp1* gene was hemizygously deleted in 5 of 8 cases of $K\text{-}ras^{LA/+}$ lung tumors with wild-type p53 (#465, #381, #154, #395, and #205).

D: Quantification of the *Dmp1* genomic DNA in lung tumors from $p53^{+/-}$ or $p53^{-/-}$; $K\text{-}ras^{LA}$ mice (mean +/− SEM). The *Dmp1* gene was not deleted in any one of these 14 lung tumors from *p53*-knockout mice.

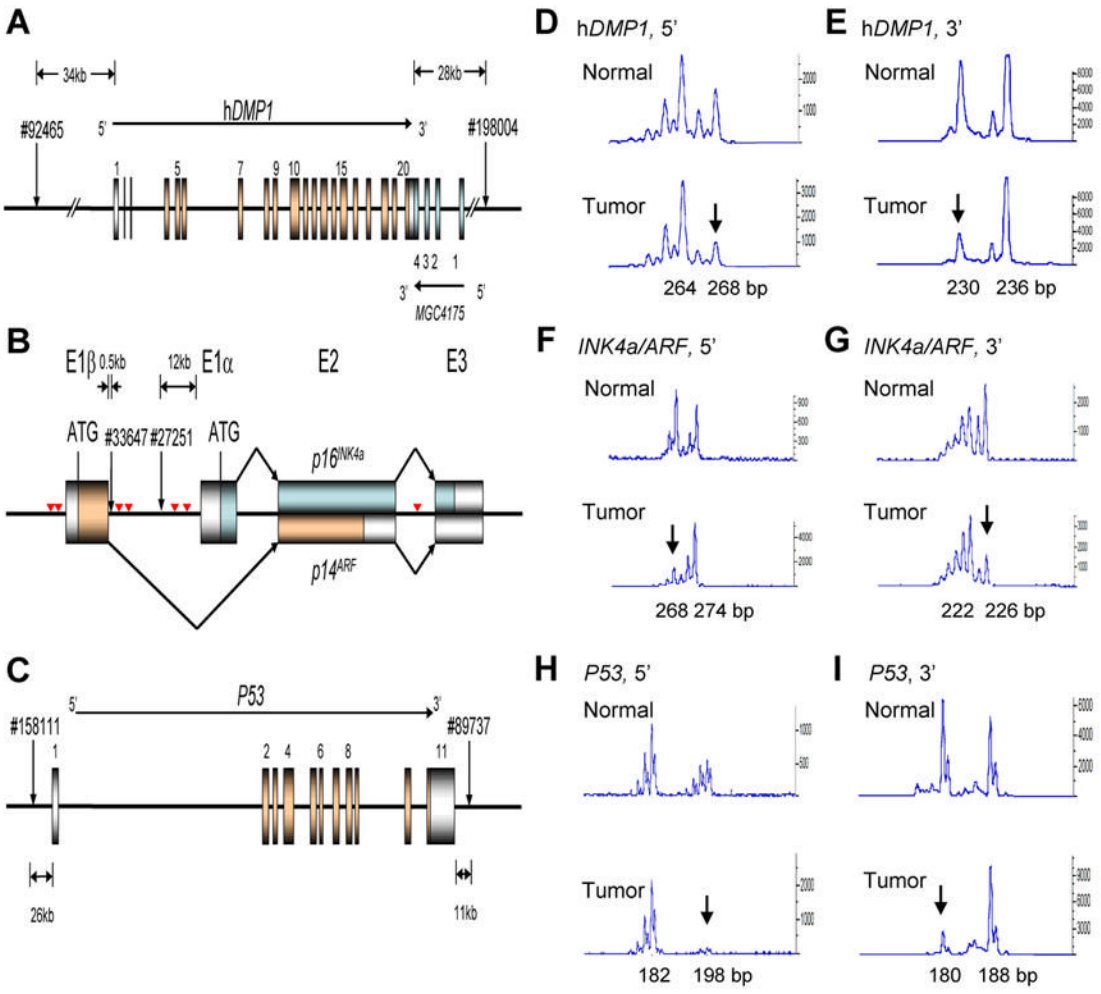

Figure 4. Loss of heterozygosity (LOH) analysis of the h*DMP1*, *INK4a/ARF*, and *P53* loci in human non-small cell lung carcinomas

A: Genomic locus of the h*DMP1* gene. The two different primer sets were designed to amplify the dinucleotide repeat sequences located on the 5' and 3' end of the h*DMP1* gene. The non-coding exons were colored silver and the coding exons were colored gold.

B: Genomic structure of the human *INK4a/ARF* locus. The two sets of PCR primers were designed to detect the dinucleotide repeats within 500 bps of Exon 1β (#33647) and those between Exon 1β and Exon 1α (#27251). The inverted triangles shown in red indicate the location of high-affinity *h*DMP1-binding sites.

C: Genomic structure of the human *P53* gene and the location of the PCR primers used for LOH analyses.

D–I: Representative patterns of LOH for *hDMP1*, *INK4a/ARF*, and *P53* in human non-small cell lung carcinoma. Genomic DNA was extracted from lung carcinomas and their normal counterparts and PCR was conducted with 6-FAM-labeled primers that amplify the dinucleotide repeats within (or close to) each locus. The area peaks of the PCR products were quantitated by ABI 3700 DNA analyzer. The qLOH values were determined through the following equation: qLOH = Area Peak 1/Area Peak 2 (normal tissue) divided by Area Peak 1'/Area Peak 2' (tumor tissue). The arrows indicate the peak that was lost in tumor cells. The sample was considered to have LOH when the value was >2.0 or <0.5.

D: LOH analysis of NSCLC with 5' h*DMP1* primer set, #92465.
E: LOH analysis of NSCLC with 3' h*DMP1* primer set, #198004.
F: LOH analysis with *INK4a/ARF* 5' probe, #33647.
G: LOH analysis with *INK4a/ARF* 3' probe, #27251.
H: LOH analysis with *P53* 5' #158111 primers.
I: LOH analysis with *P53* 3' #89737 primers.

Patient ID		hDMP1 LOH 5'	hDMP1 LOH 3'	hDMP1 Met	INK4a/ARF LOH 5'	INK4a/ARF LOH 3'	ARF Met	INK4a Met	Exclusive of DMP1 LOH	P53 LOH 5'	P53 LOH 3'	Exclusive of DMP1 LOH
1999-10	LC adeno	**0.478**	single	(-)	**0.26**	**2.29**	(-)	(-)	no	**0.29**	**0.293**	no
1999-145	LC adeno	1.13	**0.3**	(-)	0.83	0.997	(-)	(-)	yes	0.99	1.15	yes
2000-3	LC adeno	1.2	**2.08**	(+)	1.21	0.959	(-)	(-)	yes	N.D.	N.D.	
2000-19	LC adeno	1.16	**3.77**	(-)	0.98	1.12	(-)	partial	yes	1.01	single	yes
2000-20	LC adeno	single	1.27	N.D.*	single	0.708	(-)	(-)		**2.01**	**0.307**	yes
2000-21	LC adeno	1.113	1.317	(-)	single	1.354	(-)	(-)		1.339	0.824	
2000-26	LC adeno	1.3	1.24	(-)	**0.391**	**2.81**	(-)	(-)	yes	**0.178**	**0.382**	yes
2000-96	LC adeno	1.14	single	(-)	**0.497**	**>10**	(-)	(+)	yes	0.871	1.013	
2001-213	LC adeno	**2.48**	**2.39**	(-)	1.576	0.842	(-)	(-)	yes	1.056	0.71	yes
2003-38	LC adeno	**0.338**	**2.27**	N.D.	single	0.657	N.D.	N.D.	yes	N.D.	N.D.	
2003-54	LC adeno	single	0.527	(-)	0.664	**0.381**	(-)	(-)	yes	**0.16**	**>10**	yes
2003-86	LC-adeno	single	single	(-)	**del**	**0.312**	(+)	partial		**2.01**	**2.03**	
2003-304	LC adeno	1.36	1.34	(-)	1.05	1.1	(-)	partial		**2.76**	single	yes
2003-410	LC adeno	1.07	1.69	(-)	0.747	**2.19**	(-)	(-)	yes	single	**2.18**	yes
2003-422	LC adeno	0.593	0.672	(-)	**0.47**	**0.228**	partial	(+)	yes	**0.008**	**0.191**	yes
2003-442	LC adeno	single	1.29	(-)	**del**	**del**	N.D.	N.D.	yes	1.045	0.831	
2004-136	LC adeno	1.45	single	N.D.	0.88	0.66	(-)	partial		**0.47**	single	yes
2004-595	LC adeno	1.43	1.34	(-)	0.899	0.779	(-)	(-)		single	0.598	
2004-719	LC adeno	1.01	0.791	(-)	**0.223**	0.628	(-)	(+)	yes	1.519	1.26	
2004-739	LC adeno	0.95	1.23	(-)	single	0.99	(-)	(-)		0.96	1.01	
2004-983	LC adeno	1.23	single	(-)	**2.5**	**0.43**	(-)	(+)	yes	**3.03**	single	yes
2005-11	LC adeno	**0.484**	**0.488**	(-)	1.25	single	(-)	(-)	yes	**0.388**	**0.48**	no
2005-224	LC adeno	single	single	(-)	1.44	single	(-)	(-)		0.897	0.863	
2005-308	LC adeno	**2.02**	single	(-)	0.559	single	(-)	(-)	yes	**>10**	**8.16**	no
2005-391	LC adeno	0.688	single	(-)	0.696	1.006	(-)	partial		1.093	**2.45**	yes
2005-522	LC adeno	**2.01**	**0.477**	(-)	single	single	(-)	(-)		1.013	1.046	yes
2005-727	LC adeno	1.256	**2.22**	(-)	single	1.089	(-)	partial	yes	1.29	single	yes
2006-325	LC adeno	**2.3**	single	(-)	0.85	0.99	(-)	(+)	yes	0.88	0.842	yes
2006-333	LC adeno	**2.01**	0.65	(-)	1.06	0.938	(-)	partial	yes	0.52	0.57	yes
2006-416	LC adeno	1.53	0.969	(-)	single	1.18	(-)	partial		0.65	0.855	
2006-556	LC adeno	0.91	0.84	(-)	0.76	1.18	(+)	partial		**0.42**	single	yes
2006-684	LC adeno	1.21	single	(-)	1.26	0.82	(-)	partial		1.14	single	
2006-750	LC adeno	**0.49**	**>10**	(-)	1.62	1.16	(-)	(-)	yes	1.03	single	yes
1999-95	LC squam	0.766	single	(-)	**3.47**	**>10**	(-)	(+)	yes	1.805	**4.54**	yes
2000-62	LC squam	**2.49**	**2.03**	(-)	1.498	0.854	(-)	(-)	yes	0.891	0.98	yes
2002-192	LC squam	single	0.82	(-)	0.89	0.98	N.D.	N.D.		**0.25**	**2.31**	yes
2003-246	LC squam	single	0.674	(-)	**del**	0.748	(-)	(+)	yes	N.D.	N.D.	
2003-261	LC squam	**2.406**	1.22	N.D.	1.268	0.52	(-)	(-)	yes	0.62	1.396	yes
2004-593	LC squam	single	1.79	(-)	single	**0.45**	(-)	(+)	yes	1.95	**0.349**	yes
2004-707	LC squam	0.95	single	(-)	0.986	single	N.D.	(-)		1.266	1.056	
2005-83	LC squam	**0.446**	single	N.D.	0.697	1.09	(-)	(-)	yes	0.82	**0.464**	no
2005-242	LC squam	0.846	1.15	(-)	single	1.433	(-)	(+)		0.768	**0.381**	yes
2005-346	LC squam	1.026	**0.334**	(-)	1.11	single	(-)	(-)	yes	1.182	single	yes
2006-171	LC squam	single	**2.3**	(-)	0.524	0.611	(-)	(+)	yes	1.71	0.581	yes
2006-172	LC squam	1.48	single	(-)	**0.403**	**0.231**	(-)	(+)	yes	1.79	**0.271**	yes
2006-494	LC squam	0.89	single	(-)	single	**0.478**	(-)	(+)	yes	1.56	**0.122**	yes
2006-596	LC squam	**0.47**	**>10**	(-)	0.7	**0.45**	(-)	partial	no	1.1	**0.21**	no
2006-736	LC squam	0.9	0.69	(-)	1.32	**0.46**	(-)	(+)	yes	**3.05**	1.69	yes
2006-860	LC squam	**3.4**	1.42	(-)	single	1.03	(-)	(-)	yes	1.09	1.67	yes
2003-230	LC adenosq	0.89	1.43	(-)	**0.49**	**0.48**	N.D.	N.D.	yes	1.84	0.62	
2006-585	LC adenosq	1.21	1.14	(-)	0.79	0.89	(-)	partial		0.98	1.2	
Percentage		**33.3%**	**36.1%**	**2.2%**	**30.0%**	**35.6%**	**6.5%**	**53.2%**	**94.1%**	**30.4%**	**46.2%**	**85.7%**

Figure 5. Summary of the results for qLOH values and promoter hypermethylation in 51 cases of human non-small cell lung cancer

The positive results for LOH (qLOH >2.0 or <0.5) were shown in bold red characters. When one of the two markers (5' or 3') showed qLOH value >2.0 or <0.5, the sample was found to be positive for LOH for the tumor suppressor locus. Cases of mutually exclusive inactivation of h*DMP1* and *INK4a/ARF* or h*DMP1* and *P53* are shown "yes" in bold blue characters. Abbreviations: LC adeno, adenocarcinoma of the lung; LC squam, squamous cell carcinoma of the lung; LC adenosq, adenosquamous carcinoma of the lung; h*DMP1* Met, human *DMP1* promoter hypermethylation; *ARF* Met, $p14^{ARF}$ promoter hypermethylation; *INK4a* Met, $p16^{INK4a}$ promoter hypermethylation. Exclusive of DMP1 LOH, LOH of *INK4a/ARF* (or

P53) not overlapping with that of h*DMP1* in the same sample. Del, homozygous deletion; single, LOH was not evaluated due to a single peak result; partial, weak promoter methylation. N.D., not determined. N.D.*, not determined due to positive signals from histologically normal tissue (Holst et al., 2003).

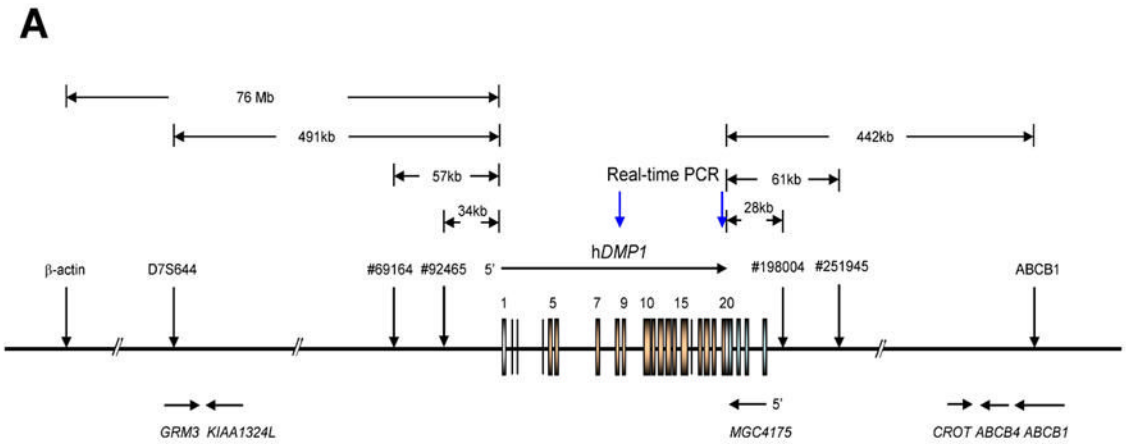

B

		LOH				Real-time PCR		LOH		
ID	Histology	B–Actin 76MB 5'	D7S644 491Kb 5'	69164, 5' 57K 5'	hDMP1 92465, 5' 34Kb 5'	Exon 8	Exon 20	hDMP1 198004,3' 28Kb 3'	251945, 3' 61Kb 3'	ABCB1 442Kb 3'
hDMP1 LOH(+) samples										
1999-10	LC adeno	1.022	1.21	1.3	**0.478**	H.D.	*no del*	*no del*	0.91	single
1999-145	LC adeno	1.08	0.98	1.17	1.13	H.D.	H.D.	**0.3**	1.13	0.98
2000-3	LC adeno	N.D.	N.D.	N.D.	1.2	H.D.	H.D.	**2.08**	N.D.	N.D.
2000-19	LC adeno	0.61	0.99	1.008	1.16	H.D.	H.D.	**3.77**	1.05	1.07
2001-213	LC adeno	0.636	**0.31**	**0.125**	**2.48**	H.D.	H.D.	**2.39**	single	1.05
2003-38	LC adeno	N.D.	**2.22**	N.D.	**0.338**	N.D.	N.D.	**2.27**	N.D.	N.D.
2005-11	LC adeno	1.028	0.64	1.312	**0.484**	H.D.	H.D.	**0.488**	**0.464**	1.69
2005-308	LC adeno	0.992	1.12	1.486	**2.02**	H.D.	*no del*	*no del*	1.95	1.48
2005-522	LC adeno	**2.2**	**2.28**	single	**2.01**	H.D.	H.D.	**0.477**	**2.05**	1.685
2005-727	LC adeno	1.04	1.05	0.813	1.256	H.D.	H.D.	**2.22**	0.725	1.13
2006-325	LC adeno	1.01	1.21	1.15	**2.3**	H.D.	*no del*	*no del*	0.817	0.83
2006-333	LC adeno	0.77	1.69	1.54	**2.01**	H.D.	*no del*	0.65	1.727	0.56
2006-750	LC adeno	0.86	**2.57**	single	**0.49**	H.D.	H.D.	**>10**	**2.95**	1.78
2000-62	LC squam	1.17	1.32	0.966	**2.49**	H.D.	*no del*	**2.03**	1.606	0.91
2003-261	LC squam	1.02	1.09	1.015	**2.406**	H.D.	H.D.	1.22	1.073	0.99
2005-83	LC squam	N.D.	1.44	0.962	**0.446**	H.D.	H.D.	*no del*	1.04	4.094
2005-346	LC squam	0.913	0.95	1.03	1.026	H.D.	H.D.	**0.334**	1.161	0.97
2006-171	LC squam	1.34	0.77	1.02	*no del*	H.D.	H.D.	**2.3**	0.907	single
2006-596	LC squam	1.1	0.85	0.74	**0.47**	H.D.	H.D.	**>10**	1.008	1.731
2006-860	LC squam	1.01	1.11	1.02	**3.4**	H.D.	H.D.	1.42	1.036	single
hDMP1 LOH(-) samples										
2000-26	LC adeno	single	0.689	0.85	1.3	*no del*	*no del*	1.24	0.906	single
2003-304	LC adeno	0.743	1.002	1.22	1.36	*no del*	*no del*	1.34	0.9	single
2004-136	LC adeno	0.96	0.775	1.17	1.45	*no del*	*no del*	*no del*	0.91	0.58
2004-719	LC adeno	1.075	1.19	0.897	1.01	*no del*	*no del*	0.791	0.844	1.21
2005-391	LC adeno	N.D.	1.36	1.1	0.688	*no del*	*no del*	*no del*	1.068	0.83
2006-684	LC adeno	1.09	1.01	0.97	1.21	*no del*	*no del*	*no del*	1.37	0.999
2006-494	LC squam	0.56	1.32	single	0.89	*no del*	*no del*	*no del*	0.55	0.88
2006-736	LC squam	0.93	0.99	1.16	0.9	*no del*	*no del*	0.69	1.04	1.08
2003-230	LC adenosq	0.75	1.08	1.002	0.89	*no del*	*no del*	1.43	1.04	single

Bold ID: ***K-Ras* mutation (+)**

hDMP1 locus

Figure 6. Detailed mapping of the chromosomal 7q21 region deleted in human NSCLC

A: Genomic structure of the human h*DMP1* locus and the primers used for the LOH analyses. GRM3: glutamate receptor 3; KIAA1324L: KIAA1324-like; MGC4175: Mammalian Gene Collection 4175; CROT: carnitine O-octanoyltransferase; ABCB4: ATP-binding cassette, sub-family B (MDR/TAP), member 4; ABCB1: ATP-binding cassette, sub-family B (MDR/TAP), member 1.

B: Summary of the qLOH and real-time PCR values with 9 different markers (7 LOH and 2 real-time PCR) in the 20 h*DMP1* LOH(+) samples and 9 h*DMP1* LOH(−) samples. The positive results for LOH (qLOH >2.0 or <0.5) are shown in bold red. In real-time PCR, the samples were found to have hemizygous deletion of h*DMP1* when the genomic DNA level was 0.25–

0.65 (H.D. in bold red, DNA in the normal lung = 1.00). The borderline cases (0.66–0.75) are shown in pink. Samples that showed point mutation for *K-Ras* at codon 12 or 13 are shown in bold ID. H.D., hemizygous deletion; *no del*, no deletion as studied by genomic DNA real-time PCR; N.D., not done; single, single peak in LOH analysis. Note that there are only two genes at the h*DMP1* locus between markers #69164 and #251945 (h*DMP1* and *MGC4175*) and this locus is selectively deleted in 15 of 19 NSCLC samples.

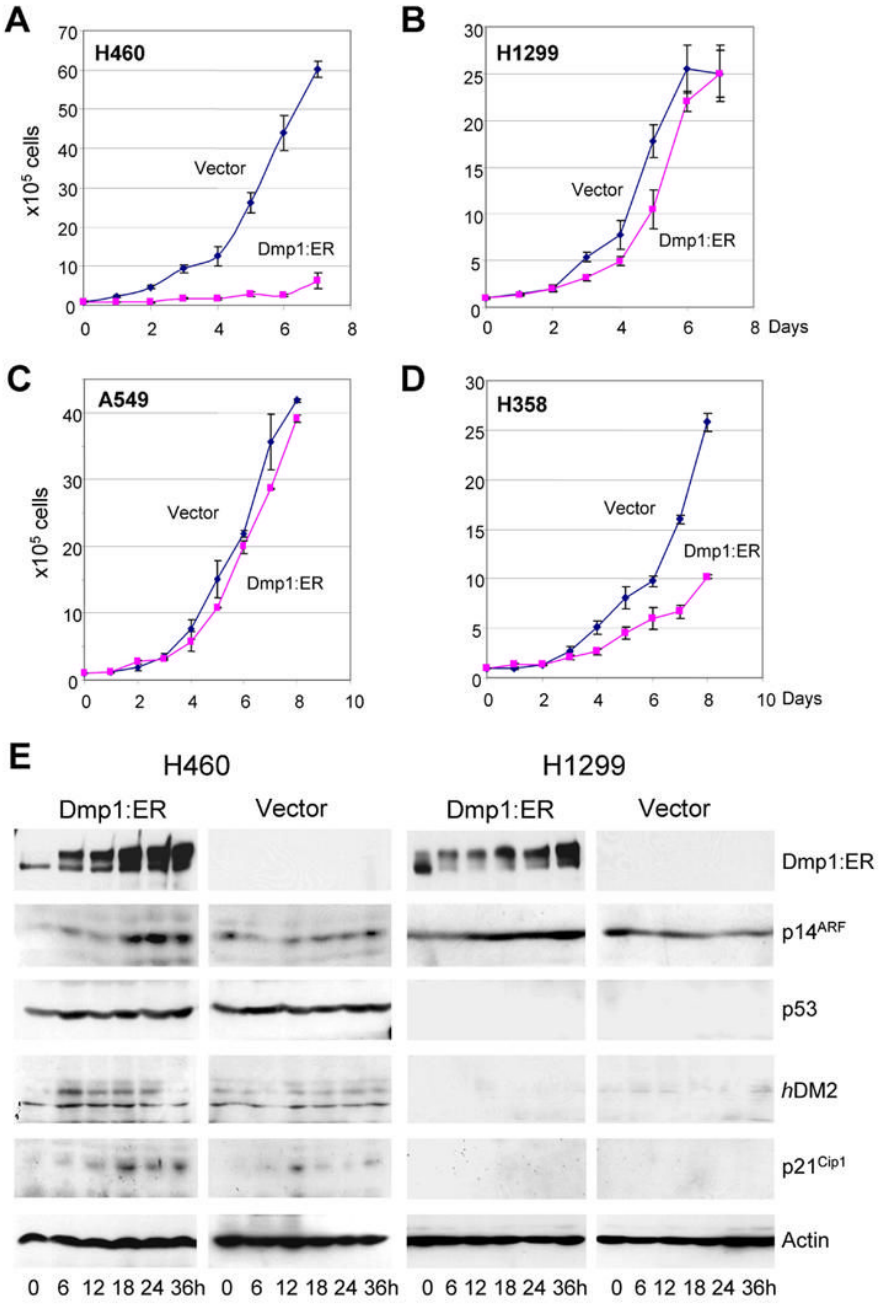

Figure 7. Proliferation assay of human non-small cell lung cancer cell lines by overexpressing Dmp1:ER

A: H460; h*DMP1*$^{+/-}$, *ARF*$^{+}$, *p16*^{del}, *P53*$^{+}$, *Rb*$^{+}$

B: H1299; h*DMP1*$^{+}$, *ARF*$^{+}$, *p16*^{Met}, *P53*^{del}, *Rb*$^{+}$

C: A549; h*DMP1*$^{+}$, *ARF*^{del}, *p16*^{del}, *P53*$^{+}$, *Rb*$^{+}$

D: H358; h*DMP1*$^{+}$, *ARF*$^{+}$, *p16*^{Met}, *P53*^{del}, *Rb*$^{+}$

Pink lines show the growth curves of Dmp1:ER virus-infected cells treated with 2μM 4-HT, blue lines show those of mock-infected cells with 4-HT (mean +/− SEM). Activation of Dmp1:ER by 4-HT inhibited the growth of H460 cells with wild-type *ARF* and *P53*, but had little effects on other lung cancer cell lines that showed deletion of *ARF* or *P53*.

E: Western blotting analyses of H460 and H1299 cells expressing activated Dmp1:ER or empty vector with specific antibodies to Dmp1, $p14^{ARF}$, p53, *h*DM2, and $p21^{Cip1}$. The numbers show hours after addition of 4-HT.